Supporting Information

Johnson et al. 10.1073/pnas.1116795108

Supporting Information Corrected November 23, 2011

SI Results

Previous biophysical studies of expressed *Caenorhabditis elegans* calcium- and voltage-activated potassium (BK) channels focused on SLO-1(A2;B0;C1), previously labeled SLO-1a (1, 2). Here, we expand the characterization of this isoform (Fig. S1). As reported previously (1), single *C. elegans* BK channels flicker rapidly between open and closed states (Fig. S1*A*, *Upper*). We measured the current carried by single channels as a function of voltage and used these data to estimate the single channel conductance, γ. The measured value, 122 pS, is smaller than that reported for vertebrate species (3) but is likely to be an underestimate owing to noise induced by the rapid channel flickering. Because such flickering precludes a detailed analysis of single-channel gating, we relied on macroscopic currents evoked by a family of voltage pulses applied to membrane patches that contained a large number of channels (Fig. S1*A*, *Lower*). Such currents reach a steady-state level within 2 ms (at 60 μM Ca^{2+}), show little to no inactivation over the pulse period (30 ms), and deactivate very rapidly.

To characterize and quantify channel activity as a function of voltage and calcium concentration and to facilitate comparisons across splice variants, we computed conductance–voltage (*G–V*) curves from the average steady-state current evoked by each voltage pulse. This procedure differs from the more common approach of using tail currents evoked by repolarization to a constant voltage. However, because *C. elegans* BK channels deactivate very rapidly at all voltages (τ <0.5 ms), it was not possible to reliably measure tail current amplitudes. In each patch, the total current amplitude depends on the size of each membrane patch and the density of functional channels in the membrane. We minimized the impact of such variation by retaining data from patches containing at least 1 nA of current at 200 mV and 60 μM calcium and normalizing *G–V* curves to the maximum conductance in each. This maneuver allows us to compare voltage sensitivity and calcium sensitivity across membrane patches and among BK channel isoforms.

Our alternative approach for deriving *G–V* curves is equivalent to the classic tail current method if and only if single-channel current amplitude varies linearly with voltage. To test whether this requirement is met, we measured the single-channel currents carried by SLO-1(A2;B0;C1) channels. We found that, similar to vertebrate BK channels, the single-channel current–voltage (*i–V*) curve in *C. elegans* was linear across a wide range of voltages (Fig. S1*B*). We assumed that a similar relationship holds for all splice variants because alternative splicing does not alter the sequence of the transmembrane domains that form the ion pore. Consistent with other BK channel homologs, lower voltages are required to activate channels exposed to increasing Ca^{2+} concentrations (Fig. S1*C*). Unlike vertebrate BK channels, however, channel opening is extremely rare in the absence of intracellular Ca^{2+} in *C. elegans*, even for voltages as high as 200 mV.

SI Materials and Methods

Reagents. Restriction enzymes and DNA-modifying enzymes were obtained from New England Biolabs. Unless indicated, reagents for PCR-based analyses were obtained from Invitrogen, nucleotide purification columns were obtained from Qiagen, primers were synthesized by Integrated DNA Technologies, and DNA sequencing of genomic DNA and cDNA plasmids was conducted by Sequetech. Unless indicated, all other chemicals were obtained from Sigma-Aldrich.

Splice Variant Identification. To discover which *slo-1* splice variants are expressed in *C. elegans*, we amplified *C. elegans slo-1* transcripts by RT-PCR over the variable region spanning exons 8–15. We used distinct primer sets to amplify splice variants that lack exon 15 (C0) or contain exon 15 (C1). In each set, the same exon 8-specific forward primer was used (5′CGGACATCAGAGTTATTGTG-C3′). The exon 15-specific reverse primer sequence was 5′GCA-AATCGAAGGGATTTCGT3′, and the exon 16-specific primer sequence was 5′AGTTTGAGCTTCTTAGTGGCA3′. We digested cDNA with restriction endonucleases that either recognized a unique site in exon 9 (A1; AlwNI) or exon 10 (A2; SalI). We purified the cDNA using a DNA filtration column and reamplified the digestion-resistant cDNA by PCR using the same primer pair used for the RT-PCR amplification step. Amplified cDNA was subcloned into pCR2.1, using the TOPO TA-cloning kit (Invitrogen) and transformed into TOP10F' *Escherichia coli* cells. We isolated plasmid DNA from individual colonies and determined whether exon 13 was absent (B0) or present in the truncated (B1) or full-length (B2) form by restriction digestion with *Hga* I, followed by gel electrophoresis. All splice-variant fragments were sequenced to confirm identity.

cDNA Constructs. We assembled full-length cDNA constructs for each splice variant. The starting material was a full-length cDNA encoding SLO-1a (A2;B0;C1) inserted into the pBluescript KS(+) vector, as reported previously (1). We substituted exon 10 (A2) for exon 9 (A1), which we amplified from a full-length *slo-1*c RT-PCR clone using the following primer pair: 5′GGCGAGATTTACT-CGCCTTC3′ (forward) and 5′TTATTGGTCCTTCGGAGTC-G3′ (reverse). We excised exon 9 contained in a restriction fragment digested by HindIII and BsmI and ligated this fragment into the *slo-1*a clone using T4 ligase. We used a similar excision and ligation strategy to generate all splice variants. We substituted all forms of exon 13 (B0, B1, and B2) from cloned *slo-1* RT-PCR fragments by excising a region spanned by BsmI and SfiI, and all forms of exon 15 (C0 and C1) by excising a region spanned by SfiI and BsiWI. All full-length splice variant cDNAs were verified by sequencing.

Heterologous Expression of BK Channel Variants in *Xenopus* Oocytes. We synthesized capped cRNAs in vitro using a mMESSAGE mMACHINE T3 kit (Ambion) and quantified yield spectroscopically. *Xenopus laevis* oocytes (Nasco) were injected with 5–50 ng cRNA per oocyte and recorded 2–5 d after injection. Oocytes were incubated at 18 °C in Hepes-buffered n-glutamine–modified Leibovitz's Medium L-15 (pH 7.4, 200 mOsM) supplemented with gentamicin (100 μg/mL).

1. Wang ZW, Saifee O, Nonet ML, Salkoff L (2001) SLO-1 potassium channels control quantal content of neurotransmitter release at the *C. elegans* neuromuscular junction. *Neuron* 32:867–881.
2. Liu Q, Chen B, Ge Q, Wang ZW (2007) Presynaptic Ca^{2+}/calmodulin-dependent protein kinase II modulates neurotransmitter release by activating BK channels at *Caenorhabditis elegans* neuromuscular junction. *J Neurosci* 27:10404–10413.
3. Hille B (2001) *Ion Channels of Excitable Membranes*, 3rd ed. (Sinauer, Sunderland, MA) chapter 12.

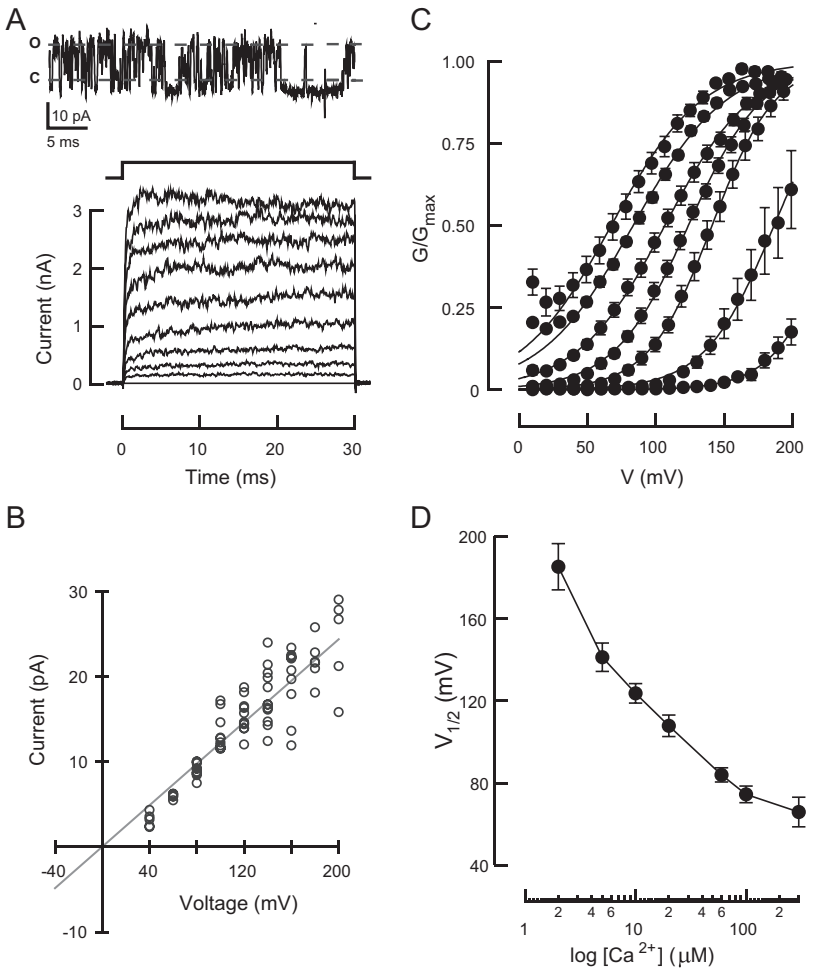

Fig. S1. Method for determining the Ca^{2+}- and voltage-dependence of *C. elegans* BK channels expressed in *Xenopus* oocytes. (*A*) Single-channel and macroscopic currents in the presence of 60 μM Ca^{2+}. (*Upper*) Representative single-channel current trace at 120 mV; dotted black lines indicate closed (C) and open (O) current levels. (*Lower*) Macroscopic currents evoked by 30-ms voltage pulses, stepping between 0 and +200 mV (in 20-mV increments) from a −80 mV holding potential. Each trace is the average of three sweeps. All recordings were filtered at 10 kHz and sampled at 100 kHz. (*B*) Single-channel current–voltage (*i–V*) relationship. Single-channel currents were measured from all-points histograms at indicated voltages and fit by a line ($r = 0.89$). Between 5 and 11 patches were analyzed at each voltage and pooled across patches exposed to Ca^{2+} concentration between 2 and 300 μM. (*C*) Normalized conductance–voltage (*G–V*) curves in the presence of decreasing Ca^{2+} concentrations (left to right): 300, 60, 20, 10, 5, 2, and 0.5 μM. Points are mean ± SEM ($n = 6$). Smooth curves were fit to the data using the Boltzmann equation. The fit parameters were ($V_{1/2}$, z): 300 μM Ca^{2+}: (77.4 ± 2.8 mV, 0.77 ± 0.06); 60 μM Ca^{2+}: (84.4 ± 1.1 mV, 0.84 ± 0.02); 20 μM Ca^{2+}: (108.4 ± 2.4 mV, 0.99 ± 0.04); 10 μM Ca^{2+}: (125.6 ± 2.3 mV, 1.05 ± 0.05); 5 μM Ca^{2+}: (141.8 ± 3.6 mV, 1.24 ± 0.07); 2 μM Ca^{2+}: (175.4 ± 6.4 mV, 1.31 ± 0.12). No fit parameters are reported for data collected in 0.5 μM Ca^{2+} because of limited channel activity under these conditions. (*D*) $V_{1/2}$ decreases as Ca^{2+} increases. Points are mean ± SEM, $n = 6$. All data are from splice variant SLO-1(A2;B0;C1).

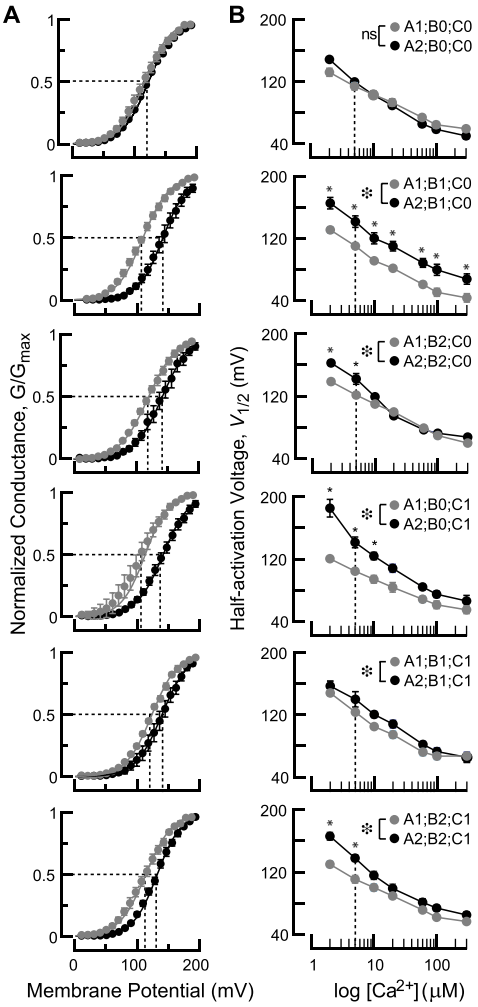

Fig. S2. Effect of alternative splicing on steady-state calcium- and voltage-dependence. (*A*) *G–V* curves for A1-type (gray) and A2-type (black) splice variants at 5 μM Ca^{2+}. Each point is the mean ± SEM ($n \geq 5$). Data were fit by the Boltzmann equation, with the following parameters ($V_{1/2}$, z): A1;B0;C0 (114.5 ± 5.8 mV, 1.24 ± 0.14); A2;B0;C0 (120.7 ± 1.6 mV, 1.21 ± 0.04); A1;B1;C0 (110.6 ± 1.6 mV, 1.21 ± 0.04); A2;B1;C0 (142.7 ± 8.1 mV, 1.28 ± 0.18); A1;B2;C0 (120.7 ± 2.0 mV, 1.10 ± 0.06); A2;B2;C0 (142.6 ± 4.7 mV, 1.15 ± 0.08); A1;B0;C1 (112.1 ± 4.0 mV, 1.32 ± 0.09); A2;B0;C1 (141.8 ± 3.6 mV, 1.24 ± 0.07); A1;B1;C1 (123.4 ± 1.4 mV, 1.22 ± 0.04); A2;B1;C1 (139.6 ± 3.67 mV, 1.20 ± 0.10); A1;B2;C1 (113.7 ± 2.0 mV, 1.19 ± 0.05); A2;B2;C1 (132.0 ± 2.3 mV, 1.32 ± 0.07). (*B*) $V_{1/2}$ decreases as Ca^{2+} increases. Points are mean ± SEM ($n \geq 5$). Significant differences between splice variant pairs were evaluated across the full Ca^{2+} concentration range by two-way ANOVAs and Bonferroni post hoc tests. Large asterisks (⁕) indicate significant main effect of the exon A variant by ANOVA ($P < 0.001$). NS, not significant ($P > 0.01$). *Significant differences ($P < 0.01$) between individual pairs of measurements for each Ca^{2+} concentration by Bonferroni post hoc tests. *F* statistics and *P* values for ANOVAs were (*Top* to *Bottom*): $F_{(1,84)} = 5.03$, $P = 0.03$ (NS); $F_{(1,62)} = 127.38$, $P < 0.001$; $F_{(1,62)} = 19.98$, $P < 0.001$; $F_{(1,68)} = 106.32$, $P < 0.001$; $F_{(1,61)} = 15.07$, $P < 0.001$; $F_{(1,80)} = 29.05$, $P < 0.001$.

Table S1. Revised splice variant nomenclature

Gene model name*	Splice variant name
slo-1a (Y51A2D.19a)	*slo-1* (A2;B0;C1)
slo-1b (Y51A2D.19b)	*slo-1* (A2;B0;C0)
slo-1c (Y51A2D.19c)	*slo-1* (A1;B1;C0)

*Gene model names are from wormbase (http://www.wormbase.org), release WS203, May 27, 2010; slo-1a, slo-1b, and slo-1c cDNAs were confirmed by sequencing (1).

Table S2. Amino acid sequence of alternate exons

Alternate exon	Amino acid sequence
A1	SPHTPLWLNDYLRGAGMEMYTESLSPSFANMSFPEAA
A2	SQTTPDWLNLYLCGAGMEMYTDTLSHSFVGMTFPEAV
B0	[skipped]
B1	——DYSDFDALFYQND
B2	KNAKISDYSDFDALFYQND
C0	[skipped]
C1	SSTSDTHLNTKSLRFAYEIKKL

Table S3. Multifactorial ANOVA analysis of the effects of alternative splicing on $z \times V_{1/2}$

Splice variant	$z \times V_{1/2}$ (mV)	*n*
A1;B0;C0	133.6 ± 8.0	9
A1;B0;C1	117.9 ± 11.7	5
A1;B1;C0	122.5 ± 9.8	5
A1;B1;C1	147.8 ± 11.8	6
A1;B2;C0	129.0 ± 8.7	5
A1;B2;C1	124.3 ± 8.9	5
A2;B0;C0	139.7 ± 12.0	5
A2;B0;C1	159.2 ± 20.3	7
A2;B1;C0	183.3 ± 16.7	6
A2;B1;C1	179.4 ± 31.0	5
A2;B2;C0	173.6 ± 24.5	6
A2;B2;C1	166.6 ± 11.9	8

Triple interaction of sites A, B, and C by multifactorial ANOVA: $F(2,60) = 6.1$, $P = 0.004$. Values are mean ± SD. Significant differences between isoforms that vary by one (-), two (=), or three (≡) splice sites ($P < 0.01$, by Tukey post hoc tests).